

Depth One Quantum Alternating Operator Ansatz as an Approximate Gibbs Distribution Sampler

Elijah Pelofske^{1,*}

¹Information Systems & Modeling, Los Alamos National Laboratory

This study numerically investigates the thermal sampling properties of QAOA, the Quantum Alternating Operator Ansatz which was generalized from the original Quantum Approximate Optimization Algorithm. Specifically, the ability of QAOA to sample from the Gibbs distribution, equivalently the Boltzmann distribution, defined by a classical Ising model, specifically a fully connected disordered spin glass (Sherrington-Kirkpatrick) model. We focus on two different QAOA mixers; the standard transverse field X mixer, and the Grover mixer. At a QAOA depth of one we examine, for a single full QAOA parameter search space period, the energy landscape, the Shannon entropy landscape of the QAOA probability distribution, and the tradeoff between Boltzmann distribution sampling temperature and error rate (how close to the true Boltzmann distribution is the QAOA distribution). We find that at very high temperatures one-round Grover mixer QAOA can sample from the Boltzmann distribution more accurately than the standard X mixer QAOA at one round. Both X mixer and Grover mixer depth one QAOA can serve as approximate Boltzmann distribution samplers, and how good this approximation is depends heavily on the QAOA angle choice.

I. INTRODUCTION

Accurate and efficient sampling from a thermal distribution (Gibbs sampling) is a foundational computational capability for information processing tasks ranging from combinatorial optimization, to statistical mechanics, to machine learning, to Bayesian statistics, and even to computational biology [1–5]. In this study, we consider the task of evaluating how well the Quantum Approximate Optimization Algorithm [6, 7] (QAOA) can sample from a Boltzmann distribution defined by a disordered classical Ising model. QAOA was later generalized to include more complicated quantum driving mechanisms, dubbed the Quantum Alternating Operator Ansatz [8]. This includes other mixing, or state transition, operations such as the XY mixers [9] and the Grover mixer [10]. Our aim is to quantify how well QAOA can sample from a particular type of complex probability distribution, in this case a Boltzmann distribution which is defined as

$$p(z) \propto e^{-\beta E(z)}, \quad (1)$$

where z is a vector of spins, $E(z)$ is the energy of that spin configuration evaluated on an Ising model, and β is the inverse temperature $\beta = 1/k_B T$. We will use natural units of the Boltzmann constant $k_B = 1$ for plotting and numerical simplicity.

QAOA is defined by several algorithmic components, which we will briefly summarize here. First, we have a cost function $C(\vec{z})$ which encodes an optimization problem we wish to solve, by finding a globally optimal assignment of spins $\vec{z} = (z_1, z_2, \dots, z_N)$, where $z \in \{+1, -1\}^n$. We will sample solutions to this optimization problem using QAOA, which involves the following components.

An initial state $|\psi\rangle$. A phase separating Hamiltonian H_P , which provides a phase shift to each basis state z according to their cost value given by $C(\vec{z})$. In other words, H_P encodes $C(\vec{z})$. A mixer Hamiltonian H_M which provides parameterized interference between basis states z . H_M is effectively the driving mechanism of QAOA by facilitating state transitions. An integer $p \geq 1$. This determines the total number of rounds of simulation are performed. Note that this parameter goes by many different terms in the literature, including *rounds*, *layers*, *levels*, and *depth*. A vector of real-values $\vec{\beta} = (\beta_1, \dots, \beta_p)$, of length p , which parameterizes H_M . A vector of real-values $\vec{\gamma} = (\gamma_1, \dots, \gamma_p)$, of length p , which parameterizes H_P .

QAOA then performs an alternating Hamiltonian simulation of these two non-commuting Hamiltonians H_P and H_M , each layer of these Hamiltonians being a parameterized quantum state, as

$$|\vec{\beta}, \vec{\gamma}\rangle = e^{-i\beta_p H_M} e^{-i\gamma_p H_P} \dots e^{-i\beta_1 H_M} e^{-i\gamma_1 H_P} |\psi\rangle. \quad (2)$$

We then measure the state $|\vec{\beta}, \vec{\gamma}\rangle$ in the computational basis to obtain a single sample. Combined, $\vec{\beta}, \vec{\gamma}$ are typically referred to as the QAOA *angles*. There is an important connection between the continuous time adiabatic quantum computation [11], and discretized digital protocols such as QAOA [12–16] – namely that fundamentally the principle being used is that long evolution times will result in high solution quality (in the case of optimization problems, this is finding globally optimal solutions, or at least close to the global minimum). In the case of QAOA, this means the number of layers p must be large in order to approach the global minimum.

Here, we will use the standard initial state of $|\psi\rangle = |+\rangle$, which provides a uniform superposition over all basis states. And we will use two different H_M Hamiltonians. The first is the standard transverse field, or X,

* epelofske@lanl.gov

mixer [6, 7]; $H_M = \sum_{i=1}^N X_i$. The other mixer we will use is the Grover mixer [10], which is based on the Grover search algorithm [17].

Note that there is a symbolic re-use collision in the thermodynamic and QAOA notation; β denotes both the QAOA mixer parameter set, and the inverse thermodynamic temperature. So as to avoid confusion, we will use $\vec{\beta}$ or $\beta_{p=1}$ to refer to the QAOA parameter, and we will use either β or β_{eff} to refer to the inverse temperature of a probability distribution.

This general sampling task of thermal state sampling goes by different terms in different fields of study. Gibbs sampling, Boltzmann sampling, and thermal sampling, all refer to the same sampling task, at least in this specific case where we sampling from a classical Hamiltonian. In the text we will interchangeably use all three of these terms.

The key motivation for this study is twofold. First, quantum algorithms such as QAOA can be implemented as very short-depth quantum circuits, making them practical to implement, albeit with noise, on current quantum computers [18–24]. Therefore, if QAOA can be a good sampler from complex probability distributions, such as Boltzmann distributions, even for moderate circuit depth (e.g., relatively small p), then those circuits could be run on current quantum computers. Second, different variants of QAOA have different thermodynamic sampling properties. Namely, Grover mixer QAOA [10] samples spin configurations that have the same cost value entirely uniformly, whereas X mixer QAOA can same configurations of the same cost non-uniformly [25–27]. In principle, this means that GM-QAOA may be a better thermal sampler, at least for some types of more frustrated Ising models, compared to the standard X mixer QAOA. Therefore, it is reasonable to analyze the differences between these two QAOA variants.

Sampling applications are one of the domains where it seems plausible that quantum computers will be able to significantly outperform classical algorithm counterparts – in the case of QAOA, there is evidence that for some QAOA trajectories and some cost functions, the output distributions are hard to approximate classically [28, 29]. An interesting open question is how the classical approximability of a QAOA probability distribution connects to how well that QAOA probability distribution approximates a Boltzmann distribution.

Literature review and prior studies– There have been a series of studies recently which have demonstrated using analog quantum computers as physical noisy samplers of a Boltzmann distribution (both quantum and classical) [30–39]. In general, there is quantum algorithmic design interest in whether quantum computers can accelerate thermal sampling computational tasks [40, 41]. The aim of this study is to examine in detail the thermal sampling properties of a very short depth digital quantum algorithm; depth one QAOA.

Refs. [42–44] have established standard QAOA can produce “pseudo-Boltzmann” states, specifically ref. [42]

used a slightly modified standard X mixer QAOA circuit to generate pseudo-Boltzmann distributions for several different types of Ising models using one QAOA round. Ref. [45] did a similar type of analysis, arguing that the standard X mixer QAOA produces approximate Boltzmann distributions – which was in part argued in the form of similar Shannon entropy between the ideal Boltzmann distribution and QAOA probability distributions. Ref. [46] compared QAOA thermal sampling and instantaneous quantum polynomial circuit thermal sampling. In the present study, the aim is to build on this line of inquiry by additionally comparing Grover mixer QAOA probability distributions. Additionally, we aim to thoroughly probe the accuracy tradeoff of depth one QAOA distributions – in other words, to quantify how close to true Boltzmann distributions, of any temperature, can these QAOA pseudo-Boltzmann states get.

Although not directly QAOA, there have been several related studies on more general variational algorithms to approximate thermal distributions. Ref. [47] proposed a variational quantum algorithm, motivated by QAOA, to prepare thermal states of different Hamiltonians including Ising models. Ref. [48] proposed a variational quantum algorithm that aims to approximate quantum Gibbs distributions. Ref. [49] used a neural network to produce approximate Boltzmann distributions, which had been trained on QAOA output distributions.

Note that this line of research is distinct from the recently proposed quantum circuit based sampler as a component of the standard iterative Markov chain Monte Carlo algorithm [50] where the sampler that is used is a short depth Trotterized quantum circuit [51, 52], equivalent to QAOA (e.g., similar idea to digitized quantum annealing [14]). In the present study, instead we investigate how well QAOA, using two different types of mixing operations, works for direct estimation of a Boltzmann distribution defined by an Ising model. In other words, this work is a numerical simulation study of the thermal sampling properties of QAOA, using two different types of non-commuting quantum Hamiltonian drivers; the standard transverse field mixer, and the Grover mixer.

II. METHODS

The Ising model we consider is a single instance of a 15-spin Sherrington-Kirkpatrick [53] (SK) model. For all edges in the fully connected 15-node graph, we randomly select either $+1$ or -1 for each local field h_i and either $+1$ or -1 for the J coupling, resulting in the spin glass Ising model of

$$\mathcal{H} = \sum_{i < j} J_{ij} \sigma_i^z \sigma_j^z + \sum_i h_i \sigma_i^z, \quad (3)$$

where σ_i^z are spins of either \uparrow or \downarrow , encoded as qubits in QAOA. Typically the goal of combinatorial optimization is to minimize the energy of this classical Hamiltonian; in

other words, find the variable assignment of the σ_i^z spins which results in a globally optimal minimum energy. The specific Ising model used in this study has a globally minimum energy of -44 , and a maximum energy of $+44$. Only a single representative Ising model is used in order to focus on and rigorously evaluate the thermal sampling properties of the QAOA across a high-resolution QAOA angle parameter search space. Considering a single, random, representative problem instance is a reasonable choice in particular for studying of the QAOA search landscape and sampling properties, of the SK model, because it is well known that QAOA control parameters concentrate strongly and perform very similarly for different instances of problems from the same class, including similar problems of very different size [20, 54–58]. This phenomenon goes by many different terms, including parameter concentration, parameter transfer, fixed point QAOA, and fixed angles, and has been analyzed on many different types of problem instances including specifically for SK models [59–65]. Therefore, it is reasonable to study the sampling properties of QAOA on small problem instances and we expect that these properties will approximately hold, due to QAOA control parameter concentration, for larger problem sizes for problems of similar types (in this case, disordered Ising models, specifically the SK model).

The quantum simulation tool which we use to compute all probabilities and expectation values is the Julia [66] based `JuliQAOA` simulator [67], which is specifically tailored for exact QAOA numerical simulation. The numerical simulations we consider are noiseless, and not represented in terms of compiled circuit models, but instead directly in the form of Hamiltonians. No qubit depolarizing error sources, or other types of error sources, are considered, and no shot noise (finite sampling effect) is considered either. The goal of this is to emphasize the noiseless thermal properties of the approximate quantum optimization algorithms. Considering finite sampling effects is an important line of study for future research.

The goal is to characterize whether certain probability distributions, in this case QAOA distributions which are parameterized by γ_1 and β_1 , result in Boltzmann distributions – or, approximations of Boltzmann distributions. However, we do not in general know what temperature QAOA may be a good Boltzmann sampler at. To this end, we perform a fitting process for different β values in order to find which value results in the lowest error. This process is performed using a combination of a β parameter gridsearch and black-box optimizers (e.g., no derivative or gradient is known a priori). This black-box optimization process still involves some statistical error, so accordingly this specifically means that there could be some β which actually gives a lower error rate than what we quantify. However, the methods we employ here attempt to minimize this statistical error as much as is reasonably possible.

We need an error rate to quantify how close to or far from the QAOA probabilities are from an ideal Boltz-

mann distribution. To this end, there are many different error measures that could be used. We will use total variation distance (TVD) which is a simple, intuitive, and bounded error measure defined for two probability distributions, $P(x)$ and $Q(x)$ as

$$\text{TVD} = \sum_x |P(x) - Q(x)|. \quad (4)$$

TVD is bounded to be between 0 ($P(x)$ and $Q(x)$ are identical), and 1 means the distributions are disjoint and have no overlap. In practice, a TVD of 0.5 is the effective maximum error that we will see between two distributions. TVD is the error measure which we will aim to minimize in the thermal distribution fitting process.

The full Boltzmann distribution fitting process involves two primary stages. The ultimate goal is to simply collect a wide range of data-points on the error rate, measured as TVD, across many inverse temperatures β . The relevant quantity we are aiming to find is that β results in the lowest TVD error rate. The first is applying black-box minimizers from `scipy` [68], namely `nelder-mead` [69], `cobyla`, `l-bfgs-b`, `powell`, `slsqp` [70], `trust-constr` [71], and `tnc`, using 28 different starting initial β guesses ranging from 10^5 to 10^{-8} . The second stage performs several grid-searches. The first is over 100 linearly spaced, in logarithmic 10 space, β values from 10^{-3} to 10^{-15} . The second is over β in steps of 10^{-4} , starting at 10^{-4} , until division by zero errors are encountered at sufficiently large β , at which point the grid-search is terminated. All TVD and β estimates are rounded to a reasonable numerical precision of 15 decimal places. Frequently, this fitting results in precision limits and division by zero errors at very low (attempted) temperature fits, all of which are discarded during this fitting process. From all of these data points, we record the minimum error rate found, and what inverse temperature β resulted in that lowest error rate – in other words, finding what β is the closest fit to the given QAOA probability distribution. This procedure is then repeated, independently, for each QAOA setting and mixer configuration. The use of the `statevector` quantum circuit simulation eliminates finite sampling effects as a consideration that must be made when determining whether the QAOA probability distribution approximates a Boltzmann distribution or not. In particular, this inverse temperature fitting may result in many possible β values that have the same TVD error rate, up to numerical TVD precision – however, this never results in high variance of the estimated β .

The full Boltzmann distribution sampling requires a significant amount of fitting and therefore computation time. To this end, we use the Python 3 libraries `Numba` and `Numpy` [72, 73] in order to significantly speed up these calculations.

Lastly, in order to quantify how uniform the QAOA probability distributions are, we turn to the Shannon entropy measure [74]

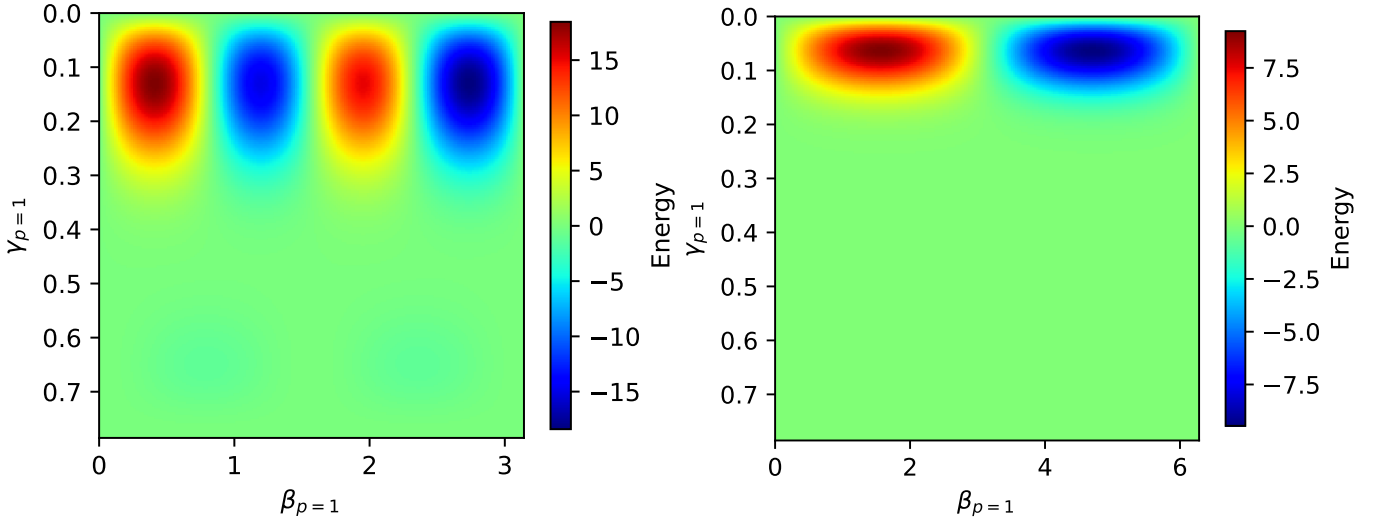


FIG. 1: Energy $p = 1$ QAOA angle landscape for the X mixer (left) and the Grover mixer (right).

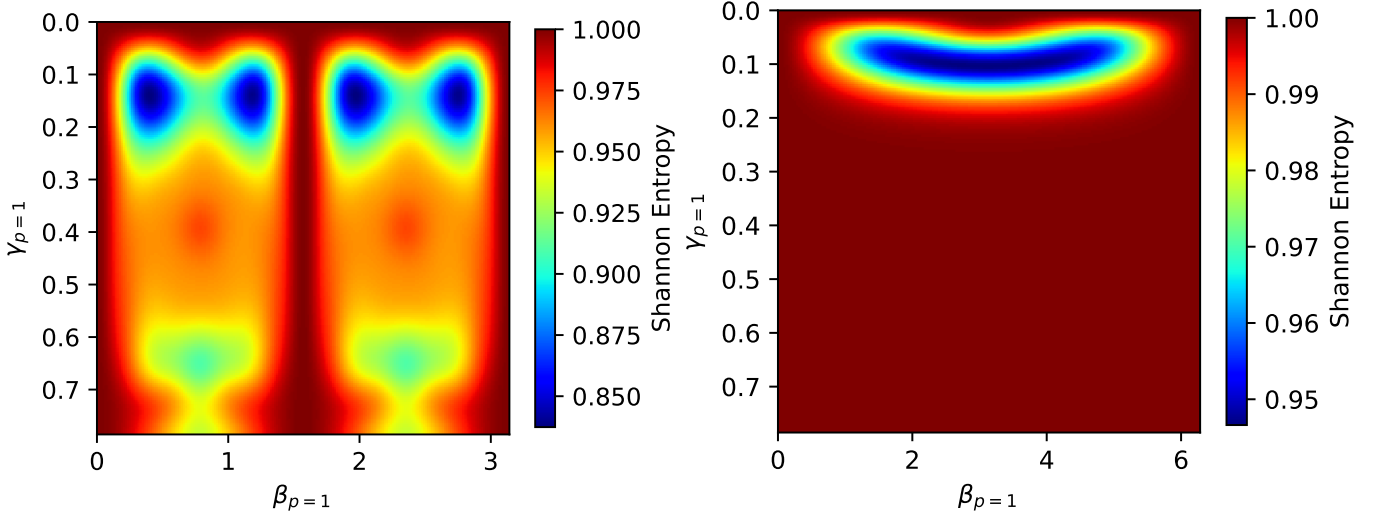


FIG. 2: Full QAOA probability distribution Shannon entropy (normalized) $p = 1$ angle landscape, for the X mixer (left) and Grover mixer (right). A Shannon entropy of 1 is the maximum possible value, corresponding to a uniform distribution, and a Shannon entropy of 0 corresponds to a maximally biased distribution.

$$S(x) = - \sum_x p(x) \log_{2^N} p(x), \quad (5)$$

where $S(x)$ is the normalized entropy (1 means a uniform distribution, and 0 means a distribution where all probabilities are on one configuration). The logarithm base is equal to the total number of configurations, which is 2^N (this gives the measure being normalized), and $p(x)$ is the (noiseless) QAOA probability of that particular z spin configuration. This information theoretic measure is another way of viewing the characteristics of these QAOA distributions; a high Shannon entropy measure across all configurations corresponds to effectively random sampling, and a lower Shannon entropy could indicate good thermal sampling (or, biased and therefore inaccurate thermal sampling).

III. RESULTS

Figure 1 presents a 200×200 QAOA energy landscape grid of $\beta_{p=1}$ and $\gamma_{p=1}$ parameters. This is where we start the thermal sampling investigation, by first simply checking the expectation value landscape. Importantly, these energies are far way from both the global minimum and maximum, so we do not expect to be sampling very low temperatures (which is reasonable, typically larger p step sizes are required in order to get to lower temperatures). Much of the angle search landscape is quite

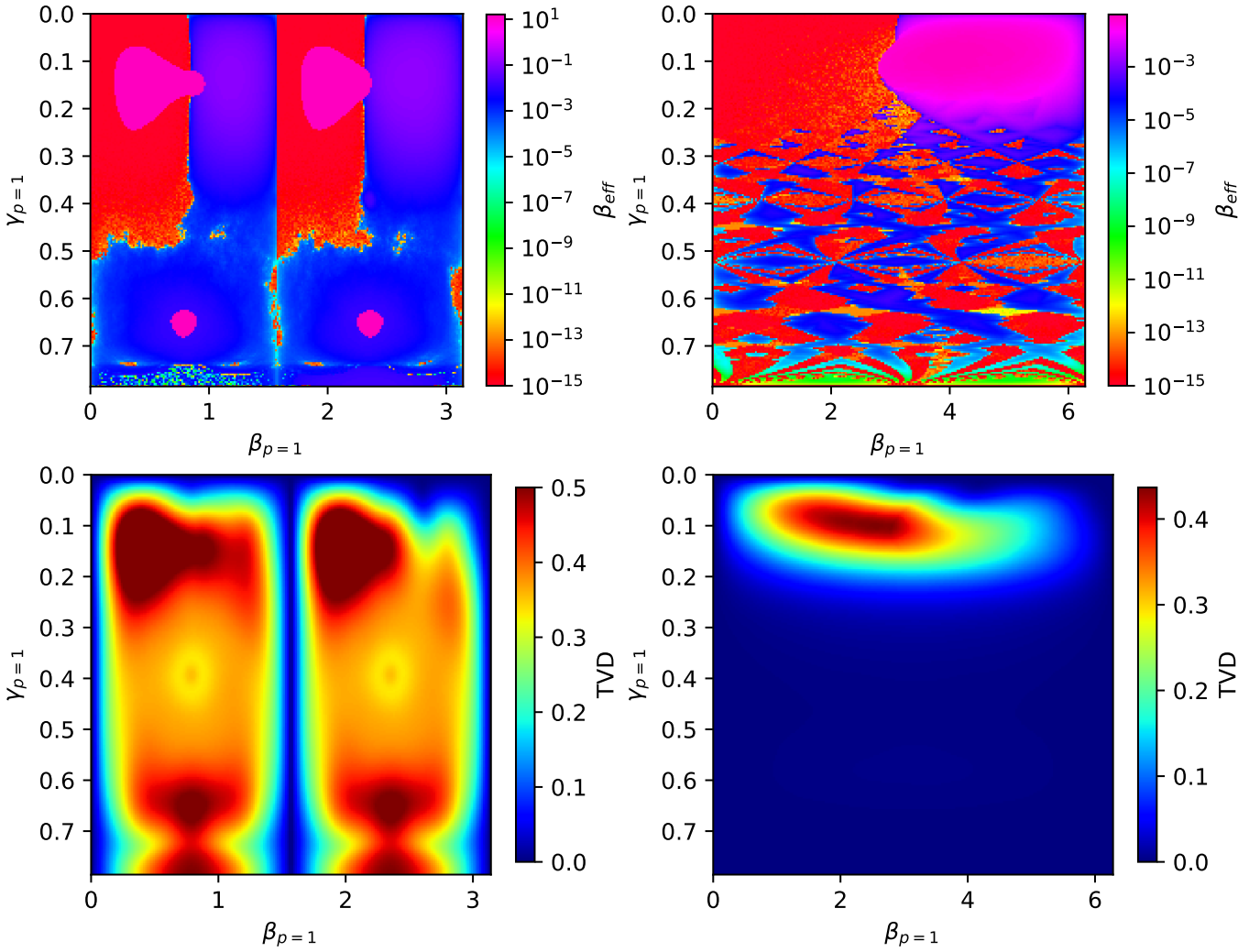


FIG. 3: Boltzmann distribution sampling properties of QAOA using the X mixer (left column) and the Grover mixer (right column). Top row contains heatmaps of the best effective inverse temperature β that was fitted to the full noiseless QAOA probability distribution, with a logarithmic scale heatmap. The bottom row contains heatmaps of the error measure, TVD, between the ideal Boltzmann distribution and the QAOA probability distribution, at the best fitted β . The TVD values, and the corresponding β value, is the absolute best-fit that was found – in other words, the lowest TVD that was found during the numerical fitting process. The heatmap landscape coordinates are given by the depth one QAOA parameters of $\vec{\gamma}$ (y-axis) and $\vec{\beta}$ (x-axis). The type of sampling that would be most interesting computationally is low temperature sampling, so maximize β . However, we also want accurate sampling, so small TVD measures – most of the low temperature sampling regimes we see in these heatmaps also have high error rates.

flat. The angle symmetries used here are a more focused and higher resolution gridsearch than the full angle periodicities – see Appendix A. Next, Figure 2 shows the Shannon entropy of the QAOA probability distributions, which show that the entropy is symmetric regardless of the expectation value (comparing to Figure 1), but also does not deviate very significantly from a nearly uniform entropy (the minimum possible entropy measure here is 0). Moreover, GM-QAOA has an higher overall configuration Shannon entropy than X mixer QAOA.

Next we turn to the fitted Boltzmann distribution

data, summarized in Figure 3. This figure shows side by side both the effective fitted inverse temperatures, and the corresponding lowest error rates that were found in this fitting process. The log-scale heatmap of β_{eff} in Figure 3 reveals a highly complex landscape, and for GM-QAOA this landscape qualitatively shows some self-similarity regions. Comparing to TVD for X mixer QAOA, it is clear that in the regions where β_{eff} is large, the corresponding error rate is also maximized to 0.5. This is important because this shows that the regions where the energy of the Hamiltonian is strictly mini-

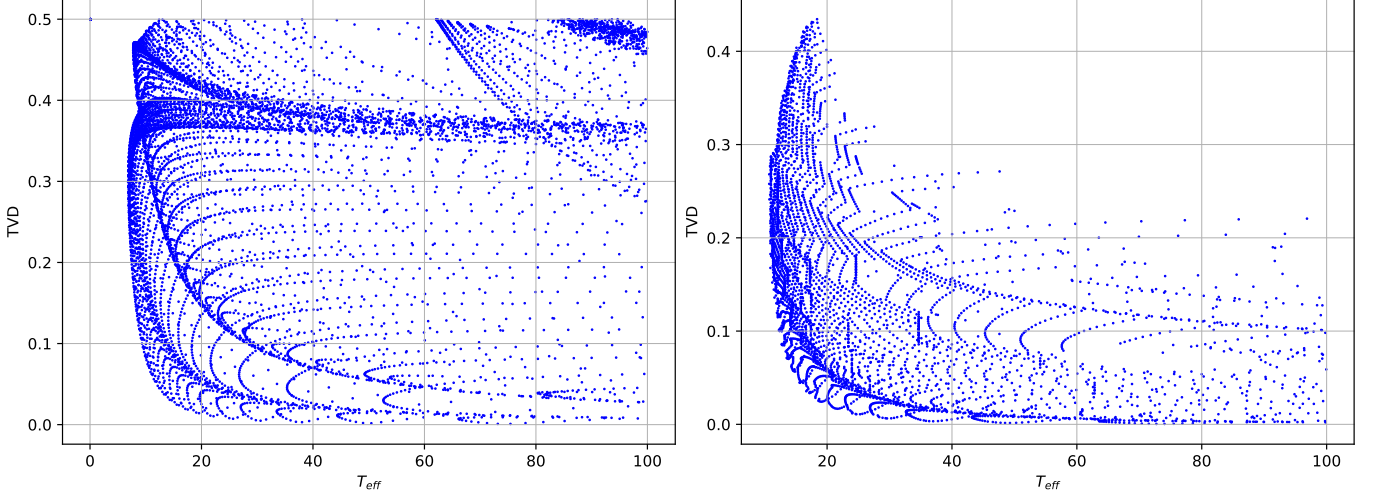


FIG. 4: Scatterplot of the TVD error (y-axis), with respect to the ideal Boltzmann distribution, of the best-fitted temperature ($1/\beta_{\text{eff}}$) found for the given QAOA sample distribution, as a function of that effective temperature (x-axis) that was fitted. X mixer QAOA distribution is shown on the left, and the Grover mixer QAOA distribution is shown on the right. TVD closer to 0 means a better approximation of the Boltzmann distribution at that effective temperature (T_{eff}). For these tradeoff plots, the aim is to focus on low temperature sampling, and therefore effective temperatures greater than 100 are not plotted. Specifically, this data is a different representation of the high resolution 200×200 grid-search plots in Figure 3, but only the points with an estimated effective temperature less than 100 are shown. We see that there are many $\vec{\beta}, \vec{\gamma}$ configurations which result in extremely high error rates of ≈ 0.5 , and for low error rates the effective temperature becomes higher.

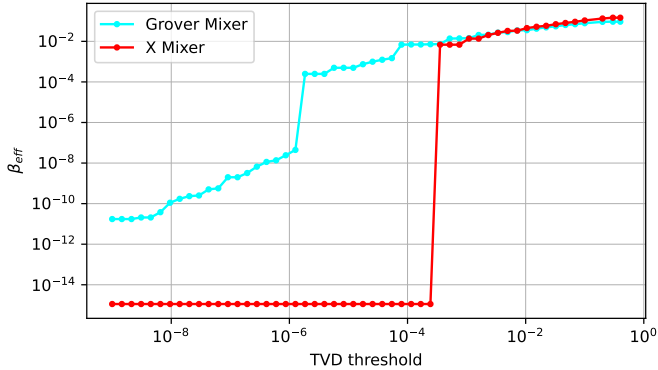


FIG. 5: Comparing the two mixers by a TVD threshold analysis where the largest effective fitted β (y-axis) that has TVD below the threshold (x-axis). logarithmic scale on both axes. We see a sharp dropoff of the X mixer sampling capability in the effective β as the TVD threshold is made smaller, whereas at very small TVD thresholds Grover mixer QAOA is able to sample at lower temperatures compared to X mixer QAOA.

mized for X mixer QAOA, the probability distributions are completely inaccurate Boltzmann distributions for that low temperature.

To more closely examine the low-error rate, low-temperature sampling region of the parameter space seen in Figure 3, next Figure 4 shows the tradeoff between the best fitted effective β and the TVD to that ideal Boltz-

Mixer, TVD error threshold	T_{eff}	$\beta_{p=1}$	$\gamma_{p=1}$
X mixer, TVD 0.1	9.32	2.6522	0.0710
X mixer, TVD 0.01	24.98	2.6206	0.0237
X mixer, TVD 0.001	73.16	2.6206	0.007893
GM mixer, TVD 0.1	12.75	4.1993	0.05131
GM mixer, TVD 0.01	28.12	4.3256	0.01973
GM mixer, TVD 0.001	70.39	4.2625	0.007893

TABLE I: Summary of some QAOA Boltzmann distribution sampling statistics, at three different TVD error rate thresholds, along with the QAOA angles that result in the thermal distribution.

mann distribution, for specific low temperature points from these QAOA angle gridsearches. We see the tradeoff illustrated clearly - where for these depth one QAOA circuits, there are no very low temperature and also low error rate QAOA probability distributions. To this end, Table I details the lowest temperature distributions that were found, under three increasingly small TVD thresholds. The trend is that as this error threshold decreases, so does the (largest) effective β that is under that threshold. Figure 5 then quantifies this in more detail by plotting what the lowest temperature (largest β) as a function of decreasingly small TVD thresholds. What we find is that there is a sharp dropoff for the X mixer around 10^{-3} TVD accuracy where the best effective β is essentially random sampling. However, for Grover mixer

QAOA, there is a more steady trend downwards, resulting in even for very small TVD thresholds, the β_{eff} is still many orders of magnitude larger than for the X mixer QAOA distributions. At very high TVD, for example at 0.3, the X mixer variant can sample at lower temperatures than GM-QAOA. This shows that GM-QAOA is a higher accuracy Gibbs distribution sampler compared to X-QAOA, at high temperatures. The reason for this could be because of the entropic properties of GM-QAOA, providing a more unbiased probability distribution for degenerate configurations in the same energy level. The reason both of the QAOA mixer variants could not achieve temperatures closer to the ground-state is because the evolution was only one-round; future work should therefore pursue studying the properties of higher depth GM-QAOA for thermal sampling.

IV. DISCUSSION AND CONCLUSION

We have demonstrated that single round QAOA can generate approximate Boltzmann distributions, and provided clear quantitative tradeoffs between temperature and accuracy, for a high resolution QAOA angle parameter search of 200×200 . We find that depth one Grover mixer QAOA can prepare more accurate Boltzmann distributions than X mixer QAOA, at relatively high temperatures. For both QAOA variants, there is a consistent tradeoff where the best-fitted lower temperature sampling also necessarily means a higher error rate. Very low error rate Boltzmann sampling can be achieved by these two depth one QAOA samplers, but only for higher temperature distributions.

Thermal state approximate sampling with relatively short depth quantum algorithms, such as QAOA, could be a good application for near term quantum computer advantage demonstrations. Further study should be done on applying GM-QAOA thermal sampling to highly frustrated magnetic models, namely systems where traditional Monte Carlo methods begin to fail.

One of the key findings of this study is that the highly optimized best performing QAOA angles, in terms of energy, are not the best Boltzmann distribution samplers – in fact, those angles result in probability distributions

that are not close to any Boltzmann distribution. This is especially true for the standard X mixer QAOA. Nevertheless, future study should perform a similar type of analysis but for higher depth QAOA circuits, using optimized QAOA angles, to assess what happens to the thermal distribution properties of QAOA in the higher depth regime.

DATA AVAILABILITY

All data from this study is publicly available as a Zenodo dataset [75].

ACKNOWLEDGMENTS

This work was supported by the U.S. Department of Energy through the Los Alamos National Laboratory. Los Alamos National Laboratory is operated by Triad National Security, LLC, for the National Nuclear Security Administration of U.S. Department of Energy (Contract No. 89233218CNA000001). Research presented in this article was supported by the NNSA’s Advanced Simulation and Computing Beyond Moore’s Law Program at Los Alamos National Laboratory. LA-UR-25-30026.

Appendix A: Full QAOA $p = 1$ Energy Landscapes

Figure 6 shows 100×100 QAOA angle landscapes, in terms of Hamiltonian energy for the full periodicity of both the phase separator and the mixing Hamiltonian. The aim here was to find what periodicities exist in this angle search range, and in particular what simplifications could be made to the angle search spaces. The result was that we used the full $[0, 2\pi]$ period for the Grover mixer angle range, and the standard $[0, \pi]$ range for the X mixer angle range. The periodicity of the γ angle was set to just $[0, \frac{\pi}{4}]$ due to the mirror symmetry we can see in Figure 6, resulting from the mirror symmetry of the Ising model. Figure 1 shows the more focused QAOA energy landscape, which was then used in all subsequent QAOA simulations.

-
- [1] H. Goto, Z. Lin, and Y. Nakamura, *Boltzmann sampling from the Ising model using quantum heating of coupled nonlinear oscillators*, *Scientific reports* **8**, 7154 (2018).
- [2] Y. Ponty, *Efficient sampling of RNA secondary structures from the Boltzmann ensemble of low-energy: the boustrophedon method*, *Journal of mathematical biology* **56**, 107–127 (2008).
- [3] P. Flajolet, É. Fusy, and C. Pivoteau, in *2007 Proceedings of the Fourth Workshop on Analytic Algorithmics and Combinatorics (ANALCO)* (SIAM, 2007) pp. 201–211.
- [4] N. Augustin, M. A. Mugglestone, and S. T. Buckland, *An autologistic model for the spatial distribution of wildlife*, *Journal of Applied Ecology* , 339–347 (1996).
- [5] C. A. Rohl, C. E. Strauss, K. M. Misura, and D. Baker, in *Methods in enzymology*, Vol. 383 (Elsevier, 2004) pp. 66–93.
- [6] E. Farhi, J. Goldstone, and S. Gutmann, *A Quantum Approximate Optimization Algorithm*, arXiv preprint (2014), [arXiv:1411.4028](https://arxiv.org/abs/1411.4028).
- [7] E. Farhi, J. Goldstone, and S. Gutmann, *A Quantum Approximate Optimization Algorithm Applied to a Bounded*

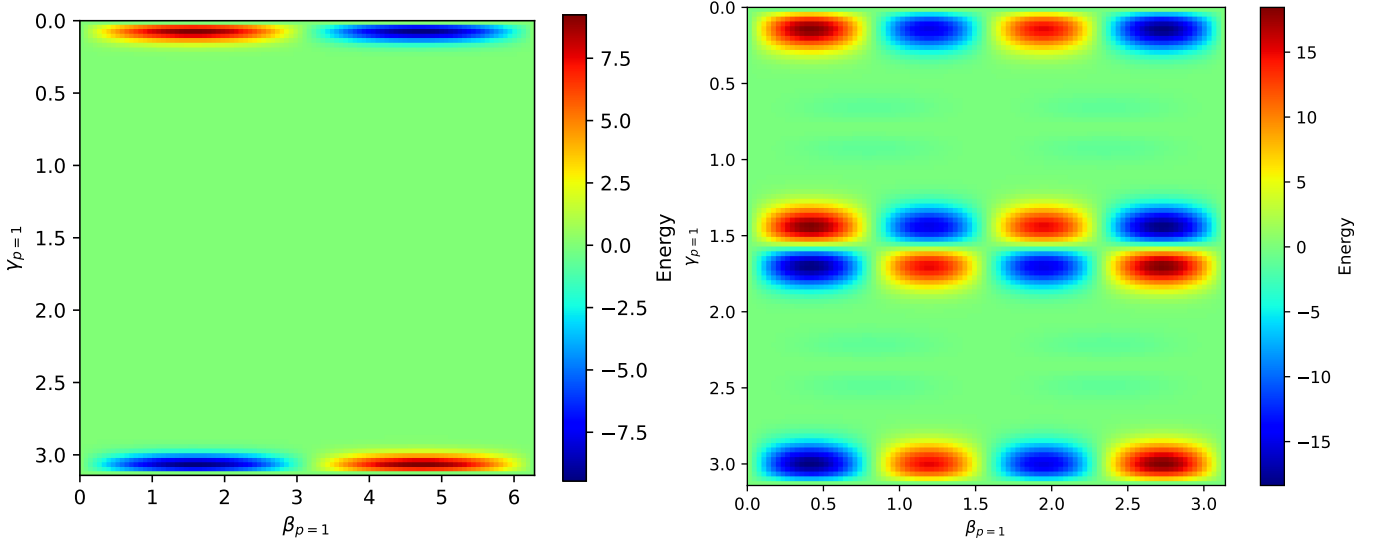


FIG. 6: Energy $p = 1$ angle landscape for the X mixer (right) and Grover mixer (left). The search landscape here is over the range of the QAOA angle symmetries for this particular SK Ising model instance, for each mixer (notice that the Grover mixer symmetry is from 0 to 2π). Using these full angle search spaces, we narrow in on smaller regions to examine for all subsequent simulations (specifically, only examining the range from $[0, \frac{\pi}{4}]$ for γ_1).

- Occurrence Constraint Problem*, arXiv preprint (2015), [arXiv:1412.6062](https://arxiv.org/abs/1412.6062).
- [8] S. Hadfield, Z. Wang, B. O'Gorman, E. Rieffel, D. Venturelli, and R. Biswas, *From the Quantum Approximate Optimization Algorithm to a Quantum Alternating Operator Ansatz*, *Algorithms* **12**, 34 (2019), [arXiv:1709.03489](https://arxiv.org/abs/1709.03489).
- [9] Z. Wang, N. C. Rubin, J. M. Dominy, and E. G. Rieffel, *XY mixers: Analytical and numerical results for the quantum alternating operator ansatz*, *Phys. Rev. A* **101**, 012320 (2020).
- [10] A. Bartschi and S. Eidenbenz, in *2020 IEEE International Conference on Quantum Computing and Engineering (QCE)* (IEEE, 2020) p. 72–82.
- [11] E. Farhi, J. Goldstone, S. Gutmann, and M. Sipser, *Quantum Computation by Adiabatic Evolution* (2000), [arXiv:quant-ph/0001106](https://arxiv.org/abs/quant-ph/0001106) [quant-ph].
- [12] S. H. Sack and M. Serbyn, *Quantum annealing initialization of the quantum approximate optimization algorithm*, *Quantum* **5**, 491 (2021), [arXiv:2101.05742](https://arxiv.org/abs/2101.05742).
- [13] S. Boulebnane, J. Sud, R. Shaydulin, and M. Pistoia, *Equivalence of Quantum Approximate Optimization Algorithm and Linear-Time Quantum Annealing for the Sherrington-Kirkpatrick Model*, arXiv preprint (2025), [arXiv:2503.09563](https://arxiv.org/abs/2503.09563).
- [14] G. B. Mbeng, R. Fazio, and G. Santoro, *Quantum Annealing: a journey through Digitalization, Control, and hybrid Quantum Variational schemes*, arXiv preprint (2019), [arXiv:1906.08948](https://arxiv.org/abs/1906.08948).
- [15] L. K. Kovalsky, F. A. Calderon-Vargas, M. D. Grace, A. B. Magann, J. B. Larsen, A. D. Baczewski, and M. Sarovar, *Self-Healing of Trotter Error in Digital Adiabatic State Preparation*, *Physical Review Letters* **131**, 060602 (2023), [arXiv:2209.06242](https://arxiv.org/abs/2209.06242).
- [16] J. A. Montañez-Barrera and K. Michielsen, *Toward a linear-ramp QAOA protocol: evidence of a scaling advantage in solving some combinatorial optimization problems*, *npj Quantum Information* **11**, 131 (2025), [arXiv:2405.09169](https://arxiv.org/abs/2405.09169).
- [17] L. K. Grover, *A fast quantum mechanical algorithm for database search* (1996), [arXiv:quant-ph/9605043](https://arxiv.org/abs/quant-ph/9605043) [quant-ph].
- [18] Z. He, D. Amaro, R. Shaydulin, and M. Pistoia, *Performance of quantum approximate optimization with quantum error detection*, *Communications Physics* **8**, 10.1038/s42005-025-02136-8 (2025).
- [19] M. P. Harrigan, K. J. Sung, M. Neeley, K. J. Satzinger, F. Arute, K. Arya, J. Atalaya, J. C. Bardin, R. Barends, S. Boixo, M. Broughton, B. B. Buckley, D. A. Buell, B. Burkett, N. Bushnell, Y. Chen, Z. Chen, B. Chiaro, R. Collins, W. Courtney, S. Demura, A. Dunsworth, D. Eppens, A. Fowler, B. Foxen, C. Gidney, M. Giustina, R. Graff, S. Habegger, A. Ho, S. Hong, T. Huang, L. B. Ioffe, S. V. Isakov, E. Jeffrey, Z. Jiang, C. Jones, D. Kafri, K. Kechedzhi, J. Kelly, S. Kim, P. V. Klimov, A. N. Korotkov, F. Kostritsa, D. Landhuis, P. Laptev, M. Lindmark, M. Leib, O. Martin, J. M. Martinis, J. R. McClean, M. McEwen, A. Megrant, X. Mi, M. Mohseni, W. Mruczkiewicz, J. Mutus, O. Naaman, C. Neill, F. Neukart, M. Y. Niu, T. E. O'Brien, B. O'Gorman, E. Ostby, A. Petukhov, H. Putterman, C. Quintana, P. Roushan, N. C. Rubin, D. Sank, A. Skolik, V. Smelyanskiy, D. Strain, M. Streif, M. Szalay, A. Vainsencher, T. White, Z. J. Yao, P. Yeh, A. Zalcman, L. Zhou, H. Neven, D. Bacon, E. Lucero, E. Farhi, and R. Babbush, *Quantum approximate optimization of non-planar graph problems on a planar superconducting processor*, *Nature Physics* **17**, 332–336 (2021).
- [20] E. Pelofske, A. Bärtschi, L. Cincio, J. Golden, and S. Eidenbenz, *Scaling whole-chip QAOA for higher-order Ising spin glass models on heavy-hex graphs*, *npj Quantum Information* **10**, 10.1038/s41534-024-00906-w (2024).
- [21] E. Pelofske, A. Bärtschi, and S. Eidenbenz, *Short-Depth QAOA Circuits and Quantum Annealing on Higher-Order Ising Models*, *npj Quantum Information* **10**, 30

- (2024).
- [22] R. Shaydulin and M. Pistoia, *QAOA with $N \cdot p \geq 200$* (2023), arXiv:2303.02064 [quant-ph].
- [23] E. Pelofske, A. Bärtschi, and S. Eidenbenz, *Quantum Annealing vs. QAOA: 127 Qubit Higher-Order Ising Problems on NISQ Computers*, in *High Performance Computing* (Springer Nature Switzerland, 2023) p. 240–258.
- [24] J. Weidenfeller, L. C. Valor, J. Gacon, C. Tornow, L. Bello, S. Woerner, and D. J. Egger, *Scaling of the quantum approximate optimization algorithm on superconducting qubit based hardware*, *Quantum* **6**, 870 (2022).
- [25] J. Golden, A. Bärtschi, D. O’Malley, and S. Eidenbenz, *Fair Sampling Error Analysis on NISQ Devices*, *ACM Transactions on Quantum Computing* **3**, 1–23 (2022).
- [26] E. Pelofske, J. Golden, A. Bärtschi, D. O’Malley, and S. Eidenbenz, in *2021 IEEE International Conference on Quantum Computing and Engineering (QCE)* (IEEE, 2021) p. 207–217.
- [27] E. Pelofske, *Biased degenerate ground-state sampling of small Ising models with converged quantum approximate optimization algorithm*, *Physical Review E* **111**, 10.1103/physreve.111.054103 (2025).
- [28] E. Farhi and A. W. Harrow, *Quantum supremacy through the quantum approximate optimization algorithm* (2019), arXiv:1602.07674 [quant-ph].
- [29] H. Krovi, *Average-case hardness of estimating probabilities of random quantum circuits with a linear scaling in the error exponent* (2022), arXiv:2206.05642 [quant-ph].
- [30] C. Ball and T. D. Cohen, *Boltzmann distributions on a quantum computer via active cooling*, *Nuclear Physics A* **1038**, 122708 (2023).
- [31] J. Marshall, D. Venturelli, I. Hen, and E. G. Rieffel, *Power of Pausing: Advancing Understanding of Thermalization in Experimental Quantum Annealers*, *Phys. Rev. Appl.* **11**, 044083 (2019).
- [32] Z. G. Izquierdo, I. Hen, and T. Albash, *Testing a Quantum Annealer as a Quantum Thermal Sampler*, *ACM Transactions on Quantum Computing* **2**, 1–20 (2021), arXiv:2003.00361.
- [33] J. Marshall, E. G. Rieffel, and I. Hen, *Thermalization, Freeze-out, and Noise: Deciphering Experimental Quantum Annealers*, *Physical Review Applied* **8**, 10.1103/physrevapplied.8.064025 (2017).
- [34] J. Nelson, M. Vuffray, A. Y. Lokhov, and C. Coffrin, *Single-Qubit Fidelity Assessment of Quantum Annealing Hardware* (2021), arXiv:2104.03335 [quant-ph].
- [35] M. Vuffray, C. Coffrin, Y. A. Kharkov, and A. Y. Lokhov, *Programmable Quantum Annealers as Noisy Gibbs Samplers*, *PRX Quantum* **3**, 020317 (2022).
- [36] J. Nelson, M. Vuffray, A. Y. Lokhov, T. Albash, and C. Coffrin, *High-Quality Thermal Gibbs Sampling with Quantum Annealing Hardware*, *Phys. Rev. Appl.* **17**, 044046 (2022).
- [37] L. Buffoni and M. Campisi, *Thermodynamics of a quantum annealer*, *Quantum Science and Technology* **5**, 035013 (2020).
- [38] T. F. Mörstedt, W. S. Teixeira, A. Viitanen, H. Kivijärvi, M. Tiiri, M. Rasola, A. M. Gunyho, S. Kundu, L. Lattier, V. Vadimov, G. Catelani, V. Sevriuk, J. Heinsoo, J. Räbinä, J. Ankerhold, and M. Möttönen, *Rapid on-demand generation of thermal states in superconducting quantum circuits* (2024), arXiv:2402.09594 [quant-ph].
- [39] R. Sandt and R. Spatschek, *Efficient low temperature Monte Carlo sampling using quantum annealing*, *Scientific Reports* **13**, 6754 (2023).
- [40] Z. Holmes, G. Muraleedharan, R. D. Somma, Y. Subasi, and B. Şahinoğlu, *Quantum algorithms from fluctuation theorems: Thermal-state preparation*, *Quantum* **6**, 825 (2022).
- [41] D. Poulin and P. Wocjan, *Sampling from the Thermal Quantum Gibbs State and Evaluating Partition Functions with a Quantum Computer*, *Physical Review Letters* **103**, 10.1103/physrevlett.103.220502 (2009).
- [42] P. Díez-Valle, D. Porras, and J. J. García-Ripoll, *Quantum Approximate Optimization Algorithm Pseudo-Boltzmann States*, *Physical Review Letters* **130**, 10.1103/physrevlett.130.050601 (2023).
- [43] P. Díez-Valle, D. Porras, and J. J. García-Ripoll, *Connection between single-layer quantum approximate optimization algorithm interferometry and thermal distribution sampling*, *Frontiers in Quantum Science and Technology* **3**, 10.3389/frqst.2024.1321264 (2024).
- [44] P. Díez-Valle, F. J. Gómez-Ruiz, D. Porras, and J. J. García-Ripoll, *Universal resources for qaoa and quantum annealing* (2025), arXiv:2506.03241 [quant-ph].
- [45] P. C. Lotshaw, G. Siopsis, J. Ostrowski, R. Herrman, R. Alam, S. Powers, and T. S. Humble, *Approximate boltzmann distributions in quantum approximate optimization*, *Phys. Rev. A* **108**, 042411 (2023).
- [46] S. Leontica and D. Amaro, *Exploring the neighborhood of 1-layer QAOA with instantaneous quantum polynomial circuits*, *Physical Review Research* **6**, 10.1103/physrevresearch.6.013071 (2024).
- [47] J. Wu and T. H. Hsieh, *Variational thermal quantum simulation via thermofield double states*, *Physical Review Letters* **123**, 10.1103/physrevlett.123.220502 (2019).
- [48] A. Warren, L. Zhu, N. J. Mayhall, E. Barnes, and S. E. Economou, *Adaptive variational algorithms for quantum gibbs state preparation* (2022), arXiv:2203.12757 [quant-ph].
- [49] Y. Nakano, K. N. Okada, and K. Fujii, *Neural-network-assisted Monte Carlo sampling trained by Quantum Approximate Optimization Algorithm* (2025), arXiv:2506.01335 [quant-ph].
- [50] N. Metropolis, A. W. Rosenbluth, M. N. Rosenbluth, A. H. Teller, and E. Teller, *Equation of state calculations by fast computing machines*, *The journal of chemical physics* **21**, 1087–1092 (1953).
- [51] D. Layden, G. Mazzola, R. V. Mishmash, M. Motta, P. Wocjan, J.-S. Kim, and S. Sheldon, *Quantum-enhanced Markov chain Monte Carlo*, *Nature* **619**, 282–287 (2023).
- [52] Y. Nakano, H. Hakoshima, K. Mitarai, and K. Fujii, *Markov-chain Monte Carlo method enhanced by a quantum alternating operator ansatz*, *Physical Review Research* **6**, 10.1103/physrevresearch.6.033105 (2024).
- [53] D. Sherrington and S. Kirkpatrick, *Solvable Model of a Spin-Glass*, *Phys. Rev. Lett.* **35**, 1792–1796 (1975).
- [54] V. Akshay, D. Rabinovich, E. Campos, and J. Biamonte, *Parameter Concentration in Quantum Approximate Optimization*, *Physical Review A* **104**, L010401 (2021), arXiv:2103.11976.
- [55] F. G. S. L. Brandao, M. Broughton, E. Farhi, S. Gutmann, and H. Neven, *For Fixed Control Parameters the Quantum Approximate Optimization Algorithm’s Objective Function Value Concentrates for Typical Instances*, arXiv preprint (2018), arXiv:1812.04170.

- [56] S. Boulebna and A. Montanaro, *Predicting parameters for the quantum approximate optimization algorithm for max-cut from the infinite-size limit*, arXiv preprint (2021), [arXiv:2110.10685](https://arxiv.org/abs/2110.10685).
- [57] R. Shaydulin, P. C. Lotshaw, J. Larson, J. Ostrowski, and T. S. Humble, *Parameter Transfer for Quantum Approximate Optimization of Weighted MaxCut*, *ACM Transactions on Quantum Computing* **4**, 19 (2023), [arXiv:2201.11785](https://arxiv.org/abs/2201.11785).
- [58] V. Katial, K. Smith-Miles, and C. Hill, *On the Instance Dependence of Optimal Parameters for the Quantum Approximate Optimisation Algorithm: Insights via Instance Space Analysis* (2024), [arXiv:2401.08142](https://arxiv.org/abs/2401.08142) [quant-ph].
- [59] J. Basso, E. Farhi, K. Marwaha, B. Villalonga, and L. Zhou, in *17th Conference on the Theory of Quantum Computation, Communication and Cryptography TQC'22* (2022) [arXiv:2110.14206](https://arxiv.org/abs/2110.14206).
- [60] R. Sakai, H. Matsuyama, W.-H. Tam, Y. Yamashiro, and K. Fujii, *Linearly simplified QAOA parameters and transferability*, arXiv preprint (2024), [arXiv:2405.00655](https://arxiv.org/abs/2405.00655).
- [61] E. Farhi, J. Goldstone, S. Gutmann, and L. Zhou, *The Quantum Approximate Optimization Algorithm and the Sherrington-Kirkpatrick Model at Infinite Size*, *Quantum* **6**, 759 (2022), [arXiv:1910.08187](https://arxiv.org/abs/1910.08187).
- [62] A. Galda, X. Liu, D. Lykov, Y. Alexeev, and I. Safro, *Transferability of optimal QAOA parameters between random graphs* (2021), [arXiv:2106.07531](https://arxiv.org/abs/2106.07531) [quant-ph].
- [63] A. Galda, E. Gupta, J. Falla, X. Liu, D. Lykov, Y. Alexeev, and I. Safro, *Similarity-Based Parameter Transferability in the Quantum Approximate Optimization Algorithm* (2023), [arXiv:2307.05420](https://arxiv.org/abs/2307.05420) [quant-ph].
- [64] A. Y. Chernyavskiy, D. A. Kulikov, B. I. Bantysh, Y. I. Bogdanov, A. K. Fedorov, and E. O. Kiktenko, *Improving QAOA to find approximate QUBO solutions in O(1) shots* (2025), [arXiv:2509.19035](https://arxiv.org/abs/2509.19035) [quant-ph].
- [65] J. Wurtz and D. Lykov, *Fixed-angle conjectures for the quantum approximate optimization algorithm on regular MaxCut graphs*, *Phys. Rev. A* **104**, 052419 (2021).
- [66] J. Bezanson, A. Edelman, S. Karpinski, and V. B. Shah, *Julia: A Fresh Approach to Numerical Computing*, SIAM review **59**, 65–98 (2017), [arXiv:1411.1607](https://arxiv.org/abs/1411.1607).
- [67] J. Golden, A. Baertschi, D. O’Malley, E. Pelofske, and S. Eidenbenz, in *Workshops of The International Conference on High Performance Computing, Network, Storage, and Analysis SC-W’23* (ACM, 2023) p. 1454–1459, [arXiv:2312.06451](https://arxiv.org/abs/2312.06451).
- [68] P. Virtanen, R. Gommers, T. E. Oliphant, M. Haberland, T. Reddy, D. Cournapeau, E. Burovski, P. Peterson, W. Weckesser, J. Bright, S. J. van der Walt, M. Brett, J. Wilson, K. J. Millman, N. Mayorov, A. R. J. Nelson, E. Jones, R. Kern, E. Larson, C. J. Carey, I. Polat, Y. Feng, E. W. Moore, J. VanderPlas, D. Laxalde, J. Perktold, R. Cimrman, I. Henriksen, E. A. Quintero, C. R. Harris, A. M. Archibald, A. H. Ribeiro, F. Pedregosa, P. van Mulbregt, and SciPy 1.0 Contributors, *SciPy 1.0: Fundamental Algorithms for Scientific Computing in Python*, *Nature Methods* **17**, 261–272 (2020).
- [69] F. Gao and L. Han, *Implementing the nelder-mead simplex algorithm with adaptive parameters*, *Comput. Optim. Appl.* **51**, 259–277 (2012).
- [70] J. Nocedal and S. J. Wright, *Numerical optimization* (Springer, 2006).
- [71] A. R. Conn, N. I. Gould, and P. L. Toint, *Trust region methods* (SIAM, 2000).
- [72] S. K. Lam, A. Pitrou, and S. Seibert, in *Proceedings of the Second Workshop on the LLVM Compiler Infrastructure in HPC*, LLVM ’15 (Association for Computing Machinery, New York, NY, USA, 2015).
- [73] C. R. Harris, K. J. Millman, S. J. van der Walt, R. Gommers, P. Virtanen, D. Cournapeau, E. Wieser, J. Taylor, S. Berg, N. J. Smith, R. Kern, M. Picus, S. Hoyer, M. H. van Kerkwijk, M. Brett, A. Haldane, J. F. del Rio, M. Wiebe, P. Peterson, P. Gérard-Marchant, K. Shepard, T. Reddy, W. Weckesser, H. Abbasi, C. Gohlke, and T. E. Oliphant, *Array programming with NumPy*, *Nature* **585**, 357–362 (2020).
- [74] C. E. Shannon, *A mathematical theory of communication*, *The Bell system technical journal* **27**, 379–423 (1948).
- [75] E. Pelofske, [10.5281/zenodo.1731607](https://doi.org/10.5281/zenodo.1731607) (2025).